Metallurgical and Materials Engineering *Research paper*
Association of Metallurgical Engineers of Serbia AMES *https://doi.org/10.30544/821*

WEAR CHARACTERIZATION OF Al 7075 ALLOY HYBRID COMPOSITES

Harish R S [*], *Sreenivasa Reddy M, Kumaraswamy J*

Department of Mechanical Engineering, R. L. Jalappa Institute of Technology, Doddabalapur-561203, Bangalore Rural Dist., India.

Received 05.04.2022

Accepted 29.05.2022

Abstract

Aluminium alloy hybrid composites are in high demand for advanced scientific applications due to their high strength, low weight, and enhanced tribological properties. A hybrid composite of aluminium alloy (Al7075) and aluminium oxide (Al_2O_3) and E-glass shot fibres was produced using a sand moulding technique in an electric resistance furnace. The objective of this research was to look at the wear characteristics of Al7075-Al_2O_3-E-glass hybrid composites with various Al_2O_3 (3-12%) and E-glass weight percentages (2-6 percent). The sliding distance (500, 1000, and 1500 m), load (10, 20, and 30N), Al_2O_3 (3, 6, and 9 %), and E-glass (2-6 %) are the wear characteristics that are considered. Wear testing is carried out using pin-on-disc equipment (WTE 165 model, Version-EV00) in line with the Taguchi L9 orthogonal array. Taguchi analysis was done on the collected data to find SN plots. Regression analysis was done along with ANOVA to find relationships between different factors selected. In order to reduce the wear rate of hybrid composites, the optimal wear parameters are determined. As the percentage of reinforcements increased, the rate of deterioration decreased. SEM scans revealed the attachment and displacement of unintended wear debris, as well as the uniform distribution of Al_2O_3/E-glass particles.

Keywords: Al7075; hybrid composites; wear behavior; L9 Taguchi.

1. Introduction

Aluminium hybrid composites are a novel type of metal matrix composite that can meet the requirements of cutting-edge technological applications. These requirements are met by hybrid aluminium composites with enhanced mechanical properties and the potential to be manufactured at a lower cost. Due to the fact that a number of processing parameters are linked to the reinforcing particles, the performance of these materials is largely dependent on the selection of the optimal combination of reinforcing materials [1-9]. MMC refers to a wide variety of materials that are typically

[*] Corresponding author: Harish and R S, *hariish.1987@gmail.com*

composed of a metallic matrix and reinforcement for the purpose of imparting desired properties. Typically, the metal matrix has superior ductility, formability, or thermal conductivity, such as aluminium, magnesium, and their alloys. Typically, the reinforcement is a ceramic with high rigidity, good strength, high hardness, high wear resistance, and a low thermal expansion coefficient. Typical examples include SiC, Al_2O_3, and B_4C ceramics. The purpose of designing MMC is to overcome certain shortcomings of the matrix in mechanical or thermal properties without compromising too much of the advantages of the matrix. In other words, MMC utilizes the advantages of both the matrix and the reinforcement [10]. Liquid metallurgy classifies Al7075-Al_2O_3-SiC HMMCs as worn and reinforces them with Al_2O_3 (2-5%) and SiC (3-7%) particulates. As the Al_2O_3 and SiC particle content was increased, MMC wear loss was drastically reduced. SEM images reveal that the matrix has resisted plastic deformation due to the presence of hard particles that act as a barrier to dislocation and lead to an increased wear force. Using orthogonal L9 specified combination levels, the influence of Al_2O_3-SiC on the wear behavior of Al7075 is realized. Variable parameters were enhanced using variance analysis (ANOVA). The discovery indicates that the wear resistance of hybrid composites is greater than that of cast composites [11]. The Al hybrid composites are reinforced with Al_2O_3 (2, 4, and 6 percent) and SiC (3, 6, and 9 percent) particles using stir casting. Taguchi's orthogonal array L27 was employed to optimize process parameters. According to the data, increasing the proportion of hard ceramic particles improves the wear resistance of the material. According to SEM data and the oxide layer formed during wear tests, abrasion wear is the most common mechanism of wear [12]. The wear of Al composites reinforced with Al6061 red mud was studied. Al6061 was used to produce composites with red mud weight percentages of 5, 10, 15, and 20 percent via stir casting. To improve material properties, T6 heat treatment was applied to composites after fabrication. Due to the presence of hard ceramic particles in red mud, composites are more resistant to wear than cast materials [13-16]. The result is converted to the noise signal ratio (S/N) of 48.13, 31.83, and 8.77 percent, using the Taguchi method. The rate of wear is affected by the type of material, application stress, and velocity. Using the best test restrictions for the wear rate, the estimated S/N ratios were calculated, and 99.5 percent confidence levels were discovered [17-19] between the expected and actual wear rates. Using variance analysis, the wear rates of matrix (Al-2219), mono (Al/B4C), and HMMC (Al/Gr/B_4C) composites were determined. The correlation coefficients were computed using linear regression models, which were then tested for conformity. According to these data, B4C concentrations and glass distance have the greatest impact on dry glass wear, followed by load and sliding speed [20-26].

In this study, Al7075/Al_2O_3/E-glass hybrid composites were created using a sand moulding procedure to investigate wear properties. The Al alloy-based hybrid composites with varied weight percentages of E-glass in the form of short fibres and aluminium oxide (Al_2O_3) particles were made in an electric arc resistance furnace. The wear loss was calculated using the Taguchi technique, which took into account the influence of reinforcements in weight %, applied load (N), and sliding distance (m), as well as their three levels. Vortex stir casting is used to prepare different weight percentages of specimens. To analyse the wear behaviour of the hybrid composite using the Taguchi L9 orthogonal array, test specimens are manufactured according to ASTM G-99 criteria.

2. Experiment

The Taguchi technique provides a high-quality product at a low cost to the producer, allowing it to be used to eliminate variation in a process. Taguchi is an experimentation design technique that demonstrates how parameters influence the significance and variation of a process performance analysis. Taguchi test design separates and arrays process parameters and levels orthogonally. The pin-on-disc apparatus (Model: WTE 165) is utilized for experimental trials involving the sliding wear rate and L9 orthogonal array. This wear test consists of nine samples measuring 30 mm in length and 8 mm in diameter. Prior to the wear test, the samples were properly cleaned with kerosene and manufactured on a CNC lathe in accordance with ASTM G-99. Table 1 demonstrates that the process parameters for wear studies are weight percent of Al_2O_3 and E-glass reinforcements, applied load (N), and sliding distance (m), all of which are varied at three distinct levels. The wear results of hybrid composites with various S/N ratios are displayed in Table 2.

Table 1. Their levels and process parameters

Sl. No.	Parameters	Level-I	Level-II	Level-III
1	Al_2O_3 (wt. %)	3	6	9
2	Load applied (N)	10	20	30
3	E-glass (wt. %)	2	4	6
4	Sliding distance (m)	500	1000	1500

2.1 Wear test procedure

The wear test is conducted using a pin-on-disc. The pins had a diameter of 8 mm and a length of 30 mm, and were made from hybrid composite materials with varying compositions. The 165 mm in diameter and 15 mm thick steel disc had a diameter of 165 mm and a thickness of 15 mm (EN31 with a hardness of 58 to 60 HRC and a roughness value of 1m). Before testing, the wear track, alloy, and composite specimens are meticulously cleaned with acetone. On a computerized scale, the specimens are then weighed with a precision of 0.001 grams. The specimen is then mounted on the tribometer's pin holder in preparation for the wear test. Cast samples were cut, machined, and polished into specimens measuring 30 mm in length and 8 mm in diameter. During the test, the sample is pressed against a rotating steel disc with a force that acts as a counterbalance and maintains the equilibrium of the pin. The track diameter was set to 165 mm, and the parameters for the weight, sliding speed, and sliding distance were adjusted. The signal produced by this arm motion is used to determine the maximum wear. Before and after the experiment, the weight loss of each specimen was measured using an electronic scale with a single pan and an accuracy of 0.001g, after a thorough washing with acetone solution. In an evaluation of the sliding wear rate under dry conditions, three variables were adjusted for three levels: applied load, sliding speed, and sliding distance. A L9 Orthogonal array with 9 rows and 7 columns was selected based on the criterion that an orthogonal array's degree of freedom must be greater than or equal to the sum of the wear parameters, and 9 trials were conducted in accordance with the Taguchi model's run order. The model's response is the wear rate. The first column of an orthogonal array corresponds to Al_2O_3, the second to E-Glass, the third to load, and the fourth to sliding distance. The purpose of the design is to reduce the rate of deterioration.

3. Results and Discussions

The experimental wear rate was used to analyze, using the Taguchi method, the expected influence of the sliding distance, reinforcement weight percent, and applied load at three levels for each parameter on the wear rate.

Using the standard L9 orthogonal wear rate study, controlled data collection was conducted. The experimental trial settings and levels were chosen using Taguchi's methodology. Utilizing ANOVA, the influence of reinforcements, loading, and sliding distance on the wear rate was analyzed. In the analysis of wear rate, a smaller is better criterion and a similar response are used. Tables 2 and 3 illustrate the difference in permissible levels between the largest and smallest mean and S/N ratio.

Figures 1 and 2 depict the principal effect charts for the average and S/N ratio of the hybrid composite wear rate, respectively. When sliding distance is increased from 500 meters to 1500 meters, the composite material's wear rate increases. This is due to the fact that the sliding distance, followed by the applied load and the reinforcement weight percentage in composites, is the most influential factor.

Table 2. The results of the Taguchi wear test in the L9 orthogonal array with the S/N ratio.

Trial	Al_2O_3 (wt. %)	E-glass (wt. %)	Load (N)	Sliding distance (m)	Wear rate (mm^3/N-m)	S/N ratio
1	3	2	10	500	0.0586	24.6420
2	3	4	20	1000	0.0657	23.6487
3	3	6	30	1500	0.0821	21.7131
4	6	2	20	1500	0.0744	22.5685
5	6	4	30	500	0.0675	23.4139
6	6	6	10	1000	0.0524	25.6134
7	9	2	30	1000	0.0652	23.7150
8	9	4	10	1500	0.0574	24.8218
9	9	6	20	500	0.0375	28.5194

Table 3. Means wear rate of response table.

Level	Al_2O_3 (wt. %)	E-glass (wt. %)	Load (N)	Sliding Distance (m)
1	0.06880	0.06607	0.05613	0.05453
2	0.06477	0.06353	0.05920	0.06110
3	0.05337	0.05733	0.07160	0.07130
Delta	0.01543	0.00873	0.01547	0.01677
Rank	3	4	2	1

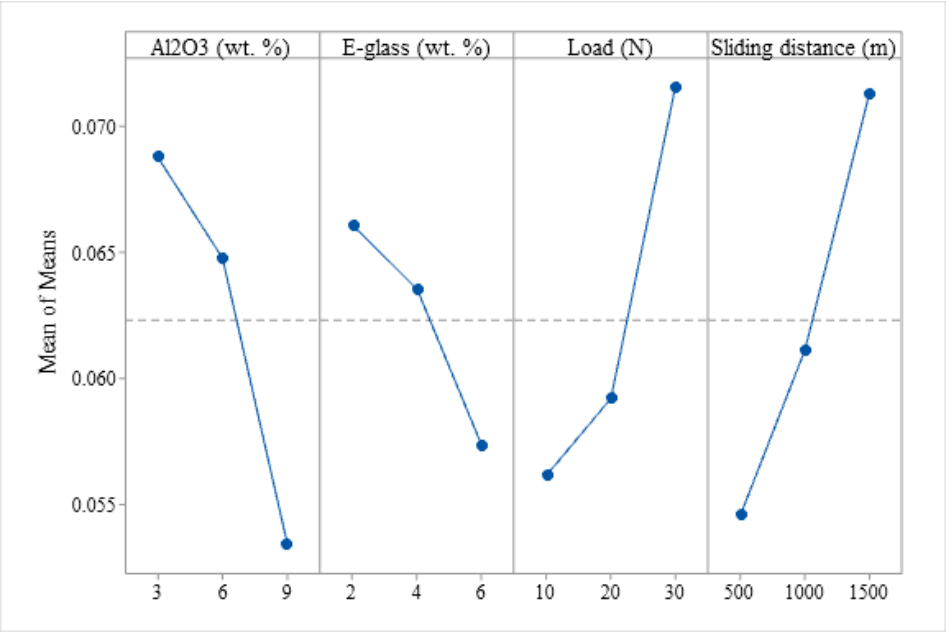

Fig. 1. Means plot of main effects.

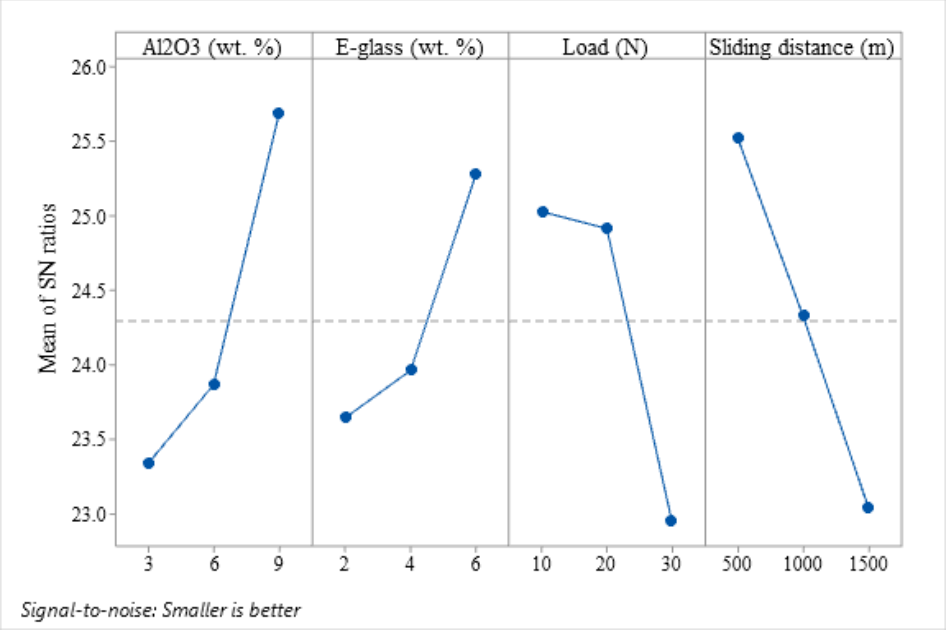

Fig. 2. S/N ratio plotted with main effects.

Table 4. Wear rate in Al7075 alloy hybrid composites was studied using ANOVA.

Source	DF	Adj. SS	Adj. MS	F-Value	P-Value	% C
Al_2O_3 (wt. %)	1	0.000357	0.000357	17.01	0.015	26.72
G-glass (wt. %)	1	0.000114	0.000114	5.45	0.080	8.53
Load (N)	1	0.000359	0.000359	17.08	0.014	26.88
Sliding Distance (m)	1	0.000422	0.000422	20.08	0.011	31.58
Error	4	0.000084	0.000021			6.29
Total	8	0.001336				100
R-Sq = 93.71%, R-Sq (Adj) = 87.43%						

Table 5. Wear rate of response table for SN ratios.

Level	Al_2O_3 (wt. %)	E-glass (wt. %)	Load (N)	Sliding Distance (m)
1	23.33	23.64	25.03	25.53
2	23.87	23.96	24.91	24.33
3	25.69	25.28	22.95	23.03
Delta	2.35	1.64	2.08	2.49
Rank	2	4	3	1

The results of the ANOVA analysis for the hybrid composite of wear behaviour are shown in Table 4. Sliding distance (31.58 %), applied load (26.88 %), and Al_2O_3 weight percent all have a significant impact on individual wear rates (26.72 %). The wear of composites is primarily determined by the sliding distance, load application, and reinforcing. Wear resistance is improved when ceramic particles are present in hybrid composites. Figure 2 shows the primary effects plot for the hybrid composite, which shows that increasing the load and sliding distance increases the wear rate of the hybrid composite. One of the key causes is that when the temperature rises, the metal surface and the base of the wear surface become softer. The composite wear rate moderately decreases as the percentage of reinforcement (hard-ceramic particles) in the alloy increases. Table 5 shows how to estimate additional reactions using analysis of variance, estimating the response for S/N ratios, and assigning the rank on S/N ratios. The most important process parameter for hybrid composites is sliding distance (Rank-1), followed by Al_2O_3 weight % (Rank-2), load (Rank-3), and E-glass weight % (Rank-4) (Rank-4).

A linear regression model fits a linear equation of the wear rate to analyse the relationship between two or more predict and response variables. The link between wear factors such Al_2O_3 weight %, E-glass weight percent, force applied, and sliding distance was investigated using linear regression models. Eq. 1 shows the wear rate regression equation for hybrid composites.

$$\textbf{Wear rate}\left(\frac{\boldsymbol{mm^3}}{\boldsymbol{N-m}}\right) = 0.05424 - 0.002572\ Al_2O_3\ (\text{wt.}\%) - 0.002183\ \text{Eglass (wt.}\%) + 0.000773\ \text{load (N)} + 0.000017\ \text{Sliding distance (m)} \quad (1)$$

3.1 Wear rate confirmation test

The experimental values were derived from experiments. The predicted value is the sum of the variables' expected values, as determined by regression analysis. When there is no difference between the data points, they are on the regression line. To verify the accuracy of wear loss, compare the predicted experimental and analytical values to the regression line depicted in Figure 3. Using regression line analysis, the accuracy of the wear rate is confirmed because the difference between the experimental and predicted values is less than 10 percent. As depicted in Figure 4, the normal probability curve for the wear rate implies that the variable parameters on either side of the curve are the same.

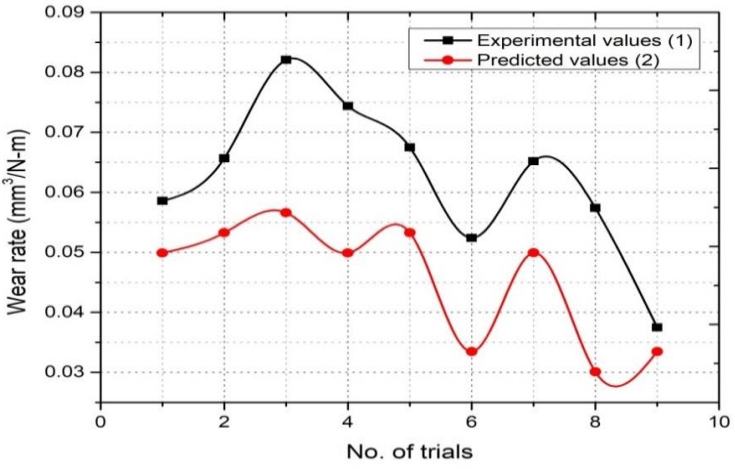

Fig. 3. Comparison of wear rates between experimental and expected values.

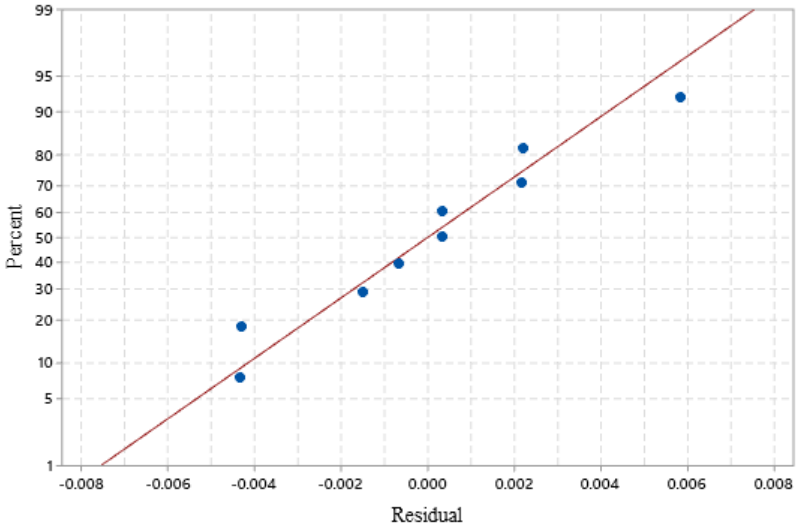

Fig. 4. Plot of normal probability.

The interaction plot in Figure 4. demonstrates how the value of the second variable component influences the association between a variable factor and a continuous response. On the x-axis, each level of one factor is represented by a line, and on the y-axis, each level of another factor is represented by a separate line. There is a positive interaction between four variable process parameters in Figure 5.

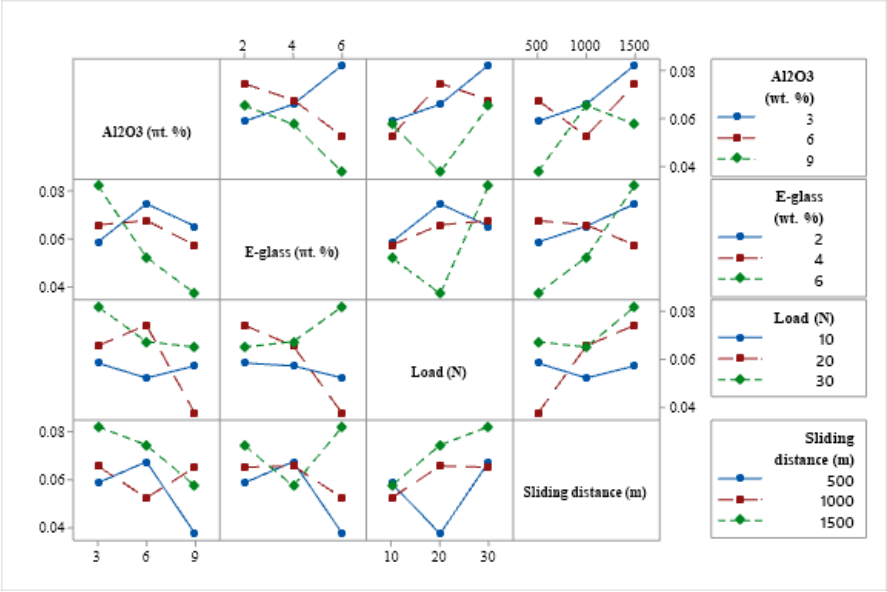

Fig. 5. Interaction plot wear rate of the composite.

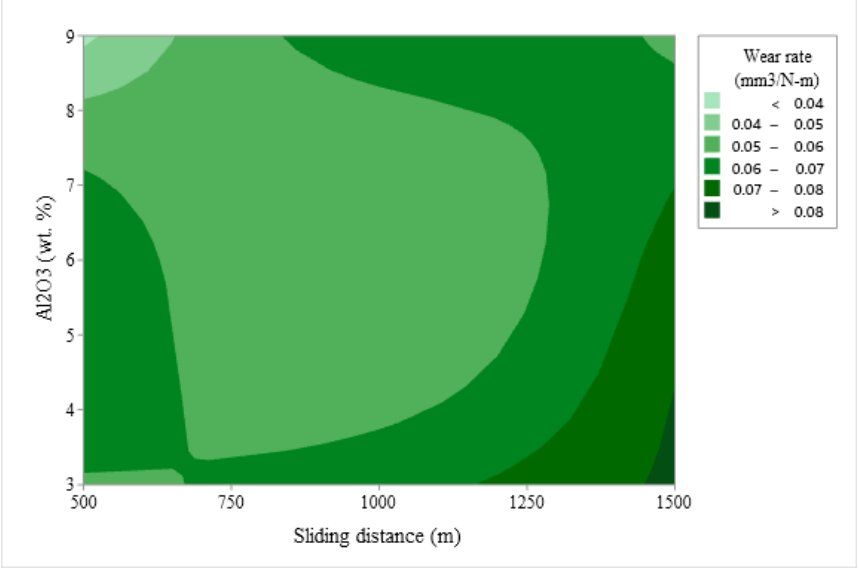

Fig. 6. Contour plot for wear rate vs. Al_2O_3 (wt. %) and sliding distance.

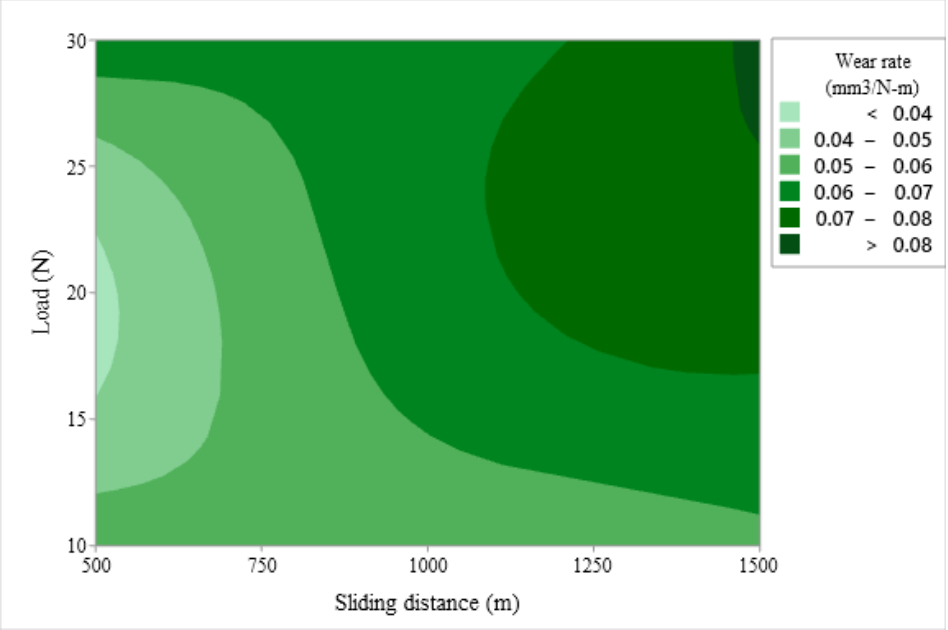

Fig. 7. Contour plots for wear rate vs. load and sliding distance.

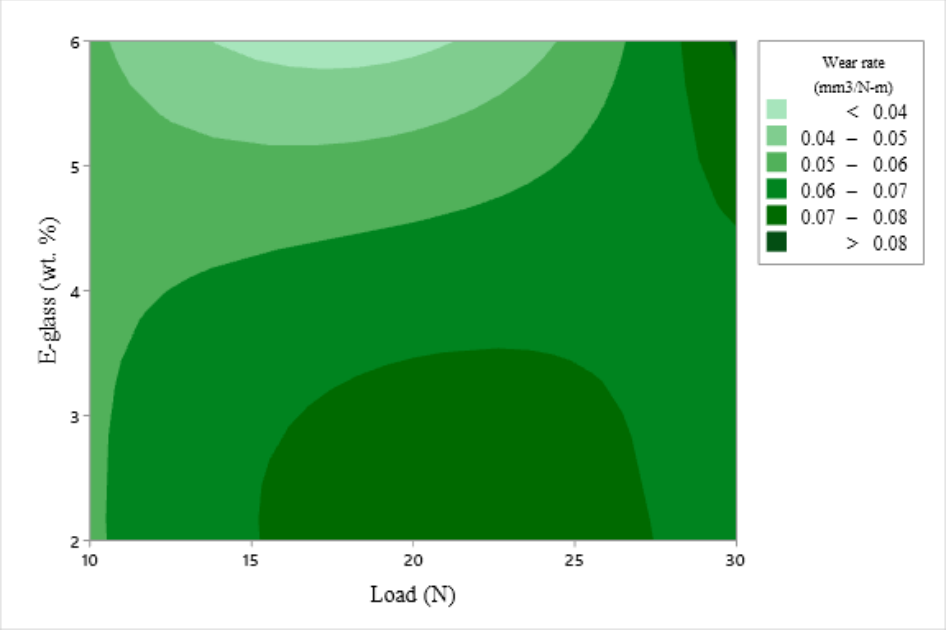

Fig. 8. Contour plot for wear rate vs. E-glass (wt. %) and load applied.

A contour plot is a two-dimensional depiction of a three-dimensional surface that requires plotting constant z-slices, or contours. Lines connect the positions (x, y) where the z value appears. As demonstrated in Figures 6 to 8, the wear rate increases as a function of the applied force and the sliding distance. Hybrid composites wear resistance improves as the percentage of hard ceramic particles in the matrix alloy increases.

3.2 Worn-out surface

SEM images of the composite specimens of worn-out surface are shown in Figure 9. The thin oxide film formed on the pin's surface when it came into contact with the disc, reducing sample wear rate. A small amount of rubbing in the sidling direction produces collateral grooves and scratches. Adhesive cold connections form at higher asperities at higher sliding speeds, and a protective oxidised layer forms on the contact surface at a short sliding distance, creating a high force on the contact surface.

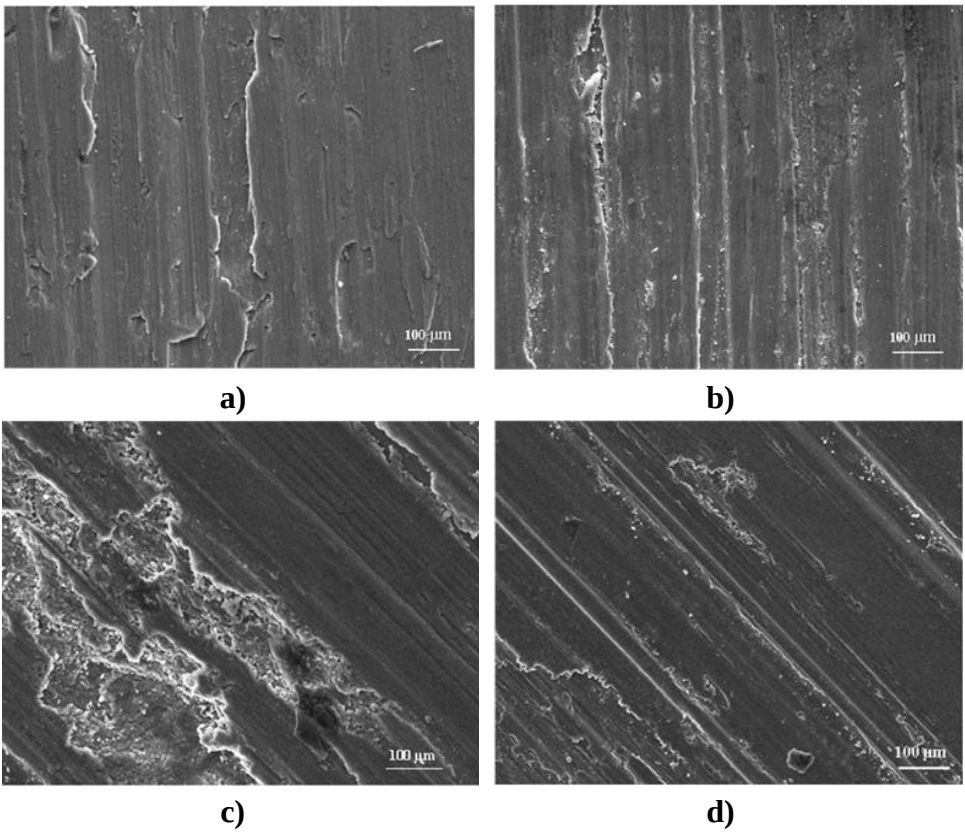

Fig. 9. Micrograph worm out surfaces: a) Al alloy + 3% Al_2O_3 + 2% E-glass at 10 N and sliding distance 500 m, b) Al alloy + 6% Al_2O_3 + 4% E-glass at 20 N and sliding distance 1000 m, c) Al alloy + 9% Al_2O_3 + 6% E-glass at 30 N and sliding distance 1500 m, d) Al alloy + 9% Al_2O_3 + 6% E-glass at 20 N and sliding distance 1500 m.

Figure 9 (a) reveals the oxidation and porous levels of sample A and the direction of the sliding speed of E-glass and Al_2O_3 with improved magnification. Figure 9 (b) shows the delamination layer of sample B and the level of grooves attained by it. Figure 9 (c) demonstrates the peeled-out position of Sample C and the oxidation level of the hybrid metal matrix composites. Figure 9 (d) shows the peeled-off position of Sample D and also provides in which direction the sliding speed of E-glass and Al_2O_3 with better magnification.

3.3 Coefficient of friction

Figure 10 depicts the average coefficient of friction of composites at different weights and velocities. As shown, the combination of Al_2O_3 and E-glass reduces the coefficient of friction for a variety of weights and speeds when used together. Under all load and speed conditions, the coefficient of friction of hybrid composites is less than that of unreinforced Al7075 alloy. For all variable loads and speeds, Al7075 alloy exhibited a high rate of COF while reinforced composites exhibited a low rate of COF. E-glass reduces the coefficient of friction by lubricating the rubbing surface with Al_2O_3, which forms a thin layer on the rubbing surface and decreases metal-on-metal contact. This indicates that Al_2O_3 in the composite acts as a surface lubricant. Consequently, it has been shown that adding Al_2O_3 and E-glass to composites improves their tribological properties.

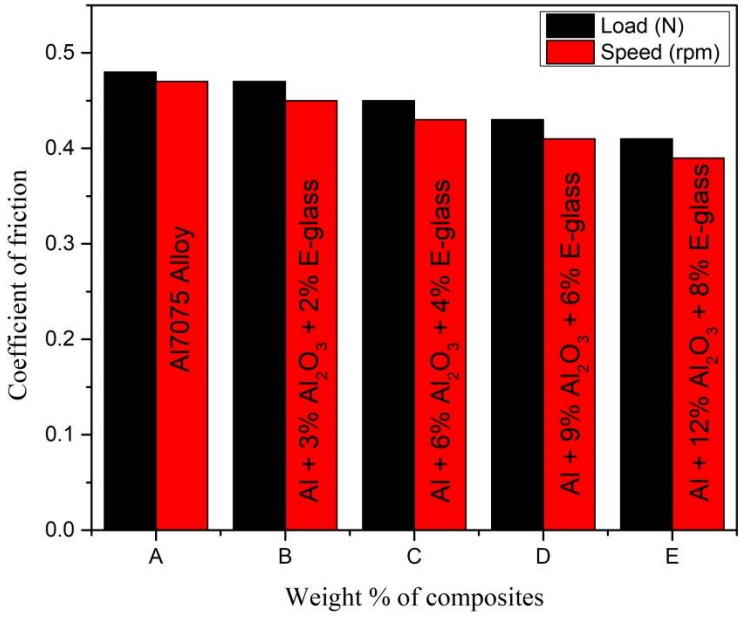

Fig.10. Friction coefficient of hybrid composites.

Conclusion

The following conclusions have been drawn as a result of the research.

As the weight percent of reinforcements (Al_2O_3/E-glass) in hybrid composites increases, the wear loss decreases. The wear rate rises as the sliding distance and weight increase.

SEM fractured surfaces study reveals a uniform distribution of Al_2O_3/ E-glass particles with the minimum amount of porosities and agglomeration. It was discovered that by combining Al_2O_3 and E-glass, a dendtrics structure is generated.

It is found that, reinforcing particles were evenly distributed in the matrix material. Reinforcing materials have attributed for the uniform wear on the as cast composite specimens of wear surface including grooves, micro cutting, and scratch marks.

The sliding distance, followed by the force applied and the reinforcing weight percentage, has the largest impact on the wear rate of hybrid composites, according to the Taguchi study.

Furthermore, the theoretical values generated from regression analysis and the experimental results are within 10% error, demonstrating that the experimental results are valid.

The coefficient of friction of hybrid composites reduced from a lower weight percentage (Al7075) to a higher weight percentage (Al7075) due to the incorporation of hard ceramic particles in the matrix alloy.

Nomenclature

Al_2O_3= Aluminium oxide,
DF= Degree of freedom,
COF= Coefficient of friction,
Wt. % = Weight percentage,
HRC = Hardness Rockwell C scale.

Acknowledgment

I would like to express my heartfelt gratitude to Dr. Sreenivasa Reddy M for his insightful suggestions and encouragement throughout the course of my research. Furthermore, I would like to thank Visvesvaraya Technological University, Jnana Sangama, Belagavi for their assistance with this project.

References

[1] M K Surappa: Sadhana, 28 (2013) 319–334.
[2] W Miller et al.: Materials Science Engineering, 280 (2000) 37–49.
[3] J Kumaraswamy, V Kumar, G Purushotham: Materials Today: Proceedings, 37 (2021) 2027–2032.
[4] Vidyasagar Shetty, Vijaya Kumar, G Purushotham: Journal of Mechanical Engineering Research and Development, 42 (2019) 231-233.
[5] Vidyasagar Shetty and B J Patil: Materials Today: Proceedings, 46 (2019) 2880-2883.
[6] K Jayappa, V Kumar, G Purushotham: Applied Science and Engineering Progress, 14 (2021) 44-51.

[7] Vidyasagar Shetty, Vijaya Kumar: International Journal of Mechanical and Production Engineering Research and Development 9 (2019) 537-544.
[8] Santosh A. Goudar, Vidyasagar Shetty: International Research Journal of Engineering and Technology, 4 (2017) 2395-0056.
[9] J Kumaraswamy, V Kumar, G Purushotham: Journal of Thermal Engineering, 7 (2021) 415-428.
[10] Ravikumar M, Reddappa H N, Suresh R, Sreenivasa reddy M: Fratturaed Integrità Strutturale, 55 (2021) 20-31.
[11] J Kumaraswamy, Vijaya Kumar, G Purushotham: International Journal of Ambient Energy, 42 (2021) 1-10.
[12] Ravikumar M et al.: Fratturaed Integrità Strutturale, 56 (2021) 160-170.
[13] Sandeep Khelge, Vijaya Kumar, Vidyasagar Shetty, J Kumaraswamy: Materials Today: Proceedings, 52 (2022) 571-576.
[14] Ravikumar M, Reddappa H N, Suresh R: Materials Today: Proceedings, 5 (2018) 5573-5579.
[15] Ravikumar M, Reddappa H N, Suresh R: Silicon, 10 (2018) 2535-2545.
[16] Sandeep Khelge, Vijaya Kumar, Kumaraswamy J: Materials Today: Proceedings, 52 (2022) 565-570.
[17] Gangadharappa M, Reddappa H N, Ravikumar M, Suresh R: Materials Today: Proceedings, 5 (2018) 22384-22389.
[18] Ugur Soy, Ferit Ficici, Adem Demir: Journal of Composite Materials, 46 (2012), 851–859.
[19] Vidyasagar Shetty, Shabari Shedthi B, J Kumaraswamy: Materials Today: Proceedings, 52(2022) 457-461.
[20] R. Suresh: Journal of the Mechanical Behaviour of Materials, 29 (2020) 57–68.
[21] Mushtaq Z., Hanief M., and Manroo S. A.: Jurnal Tribologi, 28 (2021) 117–128.
[22] Hanief M. et al.: International Journal of Nanotechnology, 18 (2021) 980–989.
[23] Anil.K.C et al.: International Journal of Science, Engineering and Management (IJSEM), 2 (2017) 29-33.
[24] Anil.K.C et al.: Materials Science and Engineering, 191 (2017) 0120-125.
[25] K.V. Sreenivas Rao et al.: Materials Today: Proceedings, Science Direct (2017) 11154–1115.
[26] Harshavardhan R, Anil K.C. K.V Sreenivas Rao, Materials Today: Proceedings 5 (2018) 24854–24861.